



Accepted Article

Title: A Mechanistic Study of the Diels-Alder Cycloaddition of C60 with Photochemically Generated Hydroxy-o-quinodimethanes.
A facile functionalization governed by steric factors

Authors: Manolis M. Roubelakis, Nikitas G Malliaros, and Michael Orfanopoulos

This manuscript has been accepted after peer review and appears as an Accepted Article online prior to editing, proofing, and formal publication of the final Version of Record (VoR). This work is currently citable by using the Digital Object Identifier (DOI) given below. The VoR will be published online in Early View as soon as possible and may be different to this Accepted Article as a result of editing. Readers should obtain the VoR from the journal website shown below when it is published to ensure accuracy of information. The authors are responsible for the content of this Accepted Article.

To be cited as: *Eur. J. Org. Chem.* 10.1002/ejoc.201900859

Link to VoR: <http://dx.doi.org/10.1002/ejoc.201900859>

A Mechanistic Study of the Diels-Alder Cycloaddition of C₆₀ with Photochemically Generated Hydroxy-*o*-quinodimethanes.

A facile functionalization governed by steric factors

Manolis M. Roubelakis,^[a] Nikitas G. Malliaros,^[a] and Michael Orfanopoulos^{*,[a]}

Dedicated to the memory of Dr. Maria Hatzimarinaki

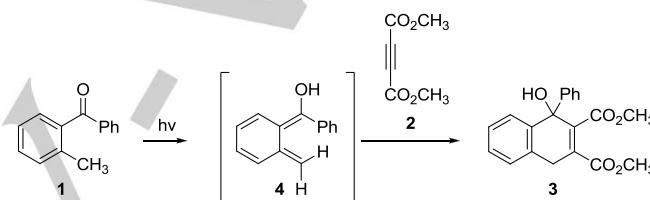
Abstract: Photoexcited *o*-alkylsubstituted benzaldehydes add to C₆₀ through their photoenol reactive intermediates producing stable [4 + 2] fullerene adducts. A mechanistic approach for this reactivity of C₆₀ is provided, based mainly on intra and intermolecular kinetic isotope effects (KIEs) studies. It is demonstrated that the rotation of C_{aromatic}-C_{carbonyl} single bond in the excited triplet state of *o*-alkyl carbonyl compounds, is the rate determining step (rds), whereas C-H(D) bond scission during the photoenolization step, occurs relatively fast.

Introduction

Diels-Alder cycloadditions are among the most common organic reactions that found application in the field of fullerene chemistry.^[1] Rigid *s-cis* dienes or dienes formed *in situ* in the presence of [60]fullerene (C₆₀) react smoothly with a [6,6] double bond on the fullerene core leading to the corresponding functionalized fullerenes, bearing a cyclohexene ring.^[1] Especially, when *o*-quinodimethanes are used as dienes, thermally stable adducts that do not revert back to the starting materials (retro-Diels-Alder) are usually formed.^[2-6] The high stability of these compounds emanates from the aromatic system generated in the final products. *o*-Quinodimethane derivatives can be obtained as intermediates either from the thermolysis of benzocyclobutenes,^[2-4] or the SO₂ extrusion of sulfolenes or sultines,^[5] or the iodide-induced 1,4-elimination of 1,2-bis-(bromomethyl)benzene derivatives,^[6] or pyrazine derivatives,^[7a] or cyclobutapyrimidines.^[7b] The efficiency of *o*-quinodimethane as the reactive intermediate in organic synthesis, has been extensively reviewed by Martín and Segura.^[8]

However, in some of the above methods the precursors are not always easily available, whereas in some other, the generation of the *o*-quinodimethane intermediates involves rather high temperatures which can lead to undesirable side reactions.

An alternative way whereby *o*-quinodimethanes that bear a hydroxy group can be accessed from alkyl substituted benzophenones was reported by Yang and Rivas.^[9] More specifically, they reported that when *o*-methylbenzophenone (**1**) is photoirradiated in the presence of a dienophile such as dimethyl acetylene-dicarboxylate (**2**), cycloadduct **3** is obtained in good yield (Scheme 1). α -Hydroxy-*o*-quinodimethane isomer **4** is formed *in situ* as the reactive intermediate of this cycloaddition.



Scheme 1. Photochemical reaction between *o*-methylbenzophenone (**1**) and dimethyl acetylene-dicarboxylate (**2**).

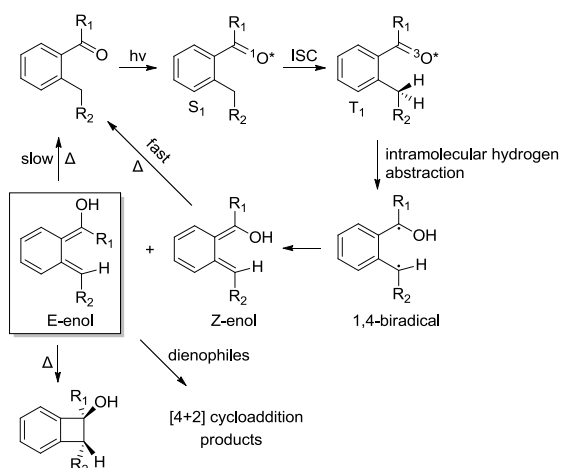
It is well-established that UV irradiation of aromatic carbonyl compounds with alkyl substituents at the *ortho* position furnishes a class of reactive intermediates, the α -hydroxy-*o*-quinodimethanes (or photoenols), through a process called photoenolization.^[10] Photoenolization mechanism is shown in Scheme 2.^[11-15]

Upon irradiation, the carbonyl group is excited to its singlet state (S₁), and then, fast intersystem crossing (ISC) furnishes the excited triplet state (T₁). This triplet state is the result of a n \rightarrow π^* carbonyl excitation and is followed by an intramolecular γ -hydrogen abstraction from the neighboring -CH₂- group leading to the formation of a triplet state 1,4-biradical intermediate (Norish Type II reaction).^[16] Eventually the biradical intermediate decays to *Z*- and *E*-enols. Of these two isomers, *Z*-enols have a very short lifetime (~100 ns) and rapidly convert back to the initial carbonyl compound via a 1,5-sigmatropic rearrangement. On the other hand, *E*-enols have significantly larger lifetimes (a few seconds) and their stereochemistry was confirmed by trapping experiments.^[10b]

Although *E*-enols partially revert to the starting material, also they can either undergo conrotatory ring closure forming cyclobutenols or can be trapped by several dienophiles, such as [60]fullerene, furnishing the corresponding [4+2] cycloaddition products (Scheme 2).

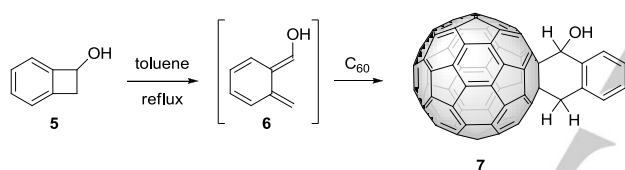
[a] Department of Chemistry, University of Crete
Voutes Campus, GR-71003
Heraklion, Crete, Greece
E-mail: morfanop@uoc.gr

Supporting information for this article is given via a link at the end of the document. **(Please delete this text if not appropriate)**



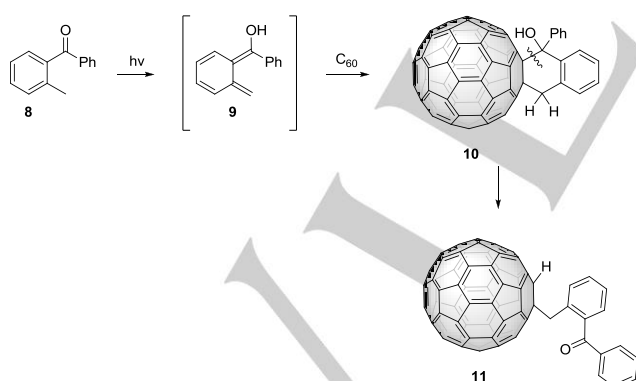
Scheme 2. The photoenolization mechanism.

The first example of a cycloaddition reaction between α -hydroxy-*o*-quinodimethanes and C_{60} was reported by Foote and coworkers.^[4] *o*-Quinodimethane (**6**) was thermally generated from benzocyclobutenol (**5**) and reacted with C_{60} to give 1,9-dihydrofullerene cycloadduct **7** (Scheme 3).



Scheme 3. Thermal cycloaddition of benzocyclobutenol with C_{60} .

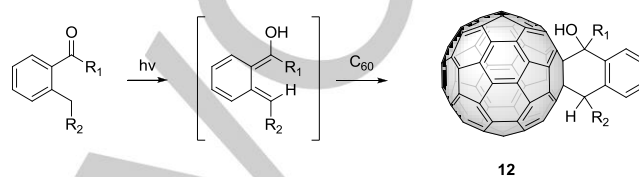
In 1995, Tomioka and coworkers for the first time tried to functionalize C_{60} with photochemically generated photoenol (**9**) derived from *o*-methylbenzophenone (**8**) (Scheme 4).^[17]



Scheme 4. Photochemical reaction of *o*-methylbenzophenone with C_{60} .

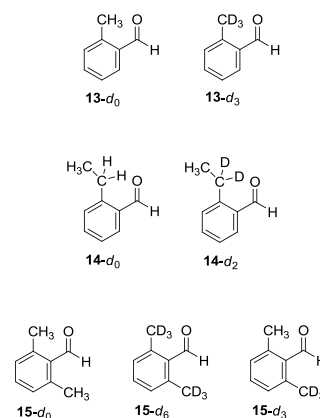
In this case, the anticipated cycloadduct **10** undergoes a facile cleavage of the $C_{fullerene}$ - $C_{benzylic}$ bond either by silica gel chromatography, or upon heating in toluene, to produce 1-(2-benzoylphenyl) methyl-1,2-dihydrofullerene (**11**).

Later on, in contrast to the instability of compound **10**, a series of quite stable fullerene derivatives (**12**) were obtained from the photolysis of commercially available *o*-tolualdehyde and related carbonyl compounds in the presence of C_{60} (Scheme 5).^[18] The successful preparation of these adducts not only established a method that overcomes synthetic difficulties of other reported methods in accessing *o*-quinodimethanes, but also, due to the presence of the hydroxyl group on the cyclohexene ring, provides the ability for further modification of the initially formed [4+2] fullerene adducts.



Scheme 5. Photochemical synthesis of [60]fullerene-*o*-quinodimethane adducts bearing a hydroxy group.

Despite the usefulness and versatility of the above reaction as well as the easiness in execution, its mechanism still remains unknown. Here we report a mechanistic study of the title Diels-Alder reaction based on the measurement of intra- and intermolecular primary and secondary H/D kinetic isotope effects (KIEs).

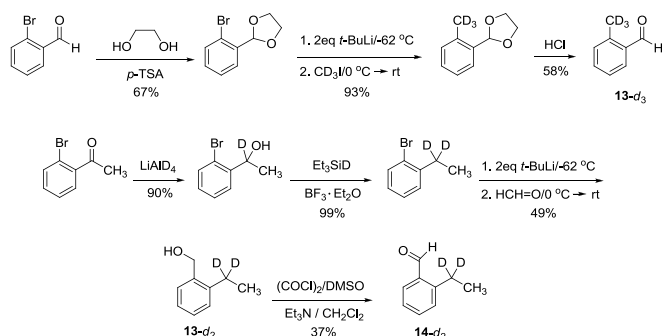


Scheme 6. Deuterated and non-deuterated substrates for the mechanistic study of the photocycloaddition reaction between C_{60} and aromatic carbonyl compounds.

o-Alkyl substituted benzaldehydes **13-d₀**, **14-d₀**, and **15-d₀** and their specifically deuterated counterparts **13-d₃**, **14-d₂**, **15-d₃** and **15-d₆**, shown in Scheme 6, were utilized for the present study. At this point it is useful to mention that although *o*-alkyl substituted ketones can also undergo similar [4+2] cycloadditions with C_{60} , through their enol intermediates, in our study we only use benzaldehydes since they react faster with C_{60} and provide higher yields.

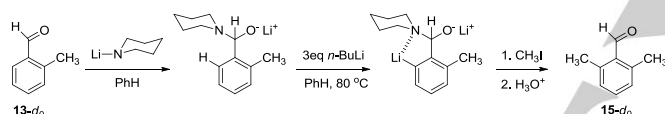
Results and Discussion

Substrates **13-d₀** and **14-d₀** are commercially available. Substrates **13-d₃** and **14-d₂** were prepared as depicted in Scheme 7 (see SI for detailed experimental procedures and spectroscopic data).



Scheme 7. Synthesis of **13-d₃** and **14-d₂**.

Compound **15-d₀** was synthesized according to a literature procedure following the route shown in Scheme 8.^[19]



Scheme 8. Synthesis of substrate **15-d₀**.

First, treatment of *o*-toluinaldehyde with lithium piperidide forms the corresponding α -amino alkoxide which is then treated with *n*-BuLi. In this intermediate alkoxide, the carbonyl group is protected against nucleophilic attack while the presence of the piperidine ring directs metalation at the 6-position due to coordination of the nitrogen atom with the Li cation. Subsequent alkylation with methyl iodide and hydrolysis provided 2,6-dimethylbenzaldehyde (**15-d₀**) in 50% yield, via a one-pot reaction.

Substrates **15-d₃** and **15-d₆** were also prepared in 48% and 50% yields respectively, following the same procedure but using deuterated methyl iodide (CD₃I) instead of CH₃I. For the synthesis of **15-d₆**, the starting material was **13-d₃**.

According to Scheme 5, the formation of [60]fullerene-*o*-quinodimethane adducts bearing a hydroxyl group seems to be a two-step reaction: first the photoenolization step that furnishes the intermediate *o*-quinodimethane and second the [4+2] cycloaddition of the reactive diene intermediate to the dienophile C₆₀. The details of the photoenolization mechanism have already been discussed above (Scheme 2). Concerning the mechanism

of the [4+2] addition of dienes and C₆₀, kinetic isotope effect studies for the reaction between rigid *s-cis* dienes and C₆₀, showed that it proceeds through a concerted pathway via a symmetrical transition state.^[20]

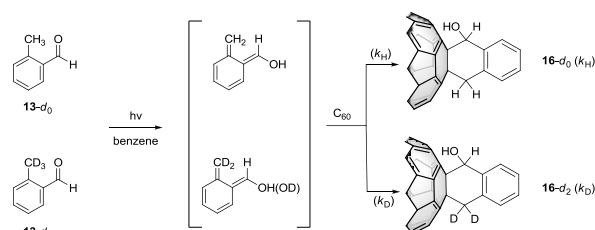
Based on this two-step reaction concept, two hypotheses can be made concerning the rate limiting step:

a) If the rate determining step of the reaction is the first one (*i.e.* photoenol formation), a normal primary isotope effect ($k_H/k_D > 1$) is expected in all cases for both the intramolecular and the intermolecular competitions. This would be the case since the photoenolization step involves a substantial C–H or C–D bond breaking in the transition state, and thus, according to the kinetic isotope effect theory the lighter isotope is favored.^[21]

b) If the rate determining step of the reaction is the second one (*i.e.* [4+2] cycloaddition), that is, the step where a rehybridization of the carbon atoms that form the 6-member ring from sp² in sp³ takes place in the transition state, then in all cases an inverse or close to unity α -secondary isotope effect is expected ($k_H/k_D \leq 1$).^[22] Again, according to the theory of kinetic isotope effects, an increase in the coordination number at the reaction center leading to a more congested transition state favors the sterically less demanding deuterium.^[21,22]

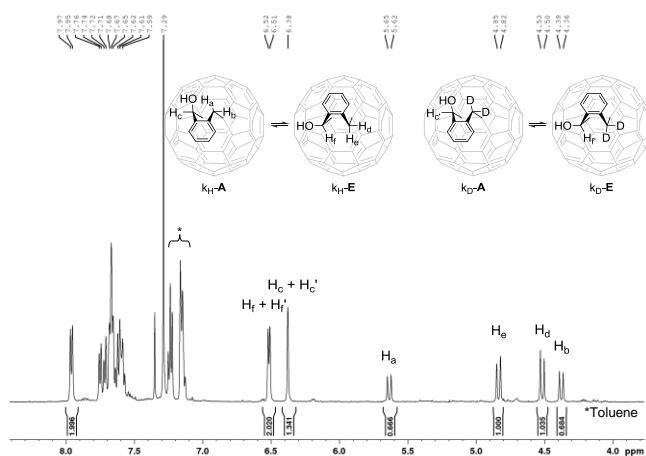
Irradiation of a mixture of C₆₀ and a 3- to 5-fold excess of substrate in benzene led to the formation of the corresponding cycloaddition adducts. The reaction progress was monitored by high performance liquid chromatography (HPLC) and the resulting products were purified by column chromatography. Intra- and intermolecular kinetic isotope effects were calculated from the ¹H NMR spectrum of the reaction products based on the integrations of the suitable peaks corresponding to k_H and k_D products (*vide infra*).

As an example, below we describe how we determined the intermolecular kinetic isotope effect for the reaction between **13-d₀**/**13-d₃** and C₆₀. The reaction that takes place when a 3-fold excess of an equimolar mixture of **13-d₀**/**13-d₃** is irradiated in the presence of C₆₀ is shown in Scheme 9.



Scheme 9. Photocycloaddition of an equimolar mixture of **13-d₀**/**13-d₃** to C₆₀.

In the two reaction products **16-d₀** (k_H) and **16-d₂** (k_D), cyclohexene ring adopts a boat conformation and as a result, at room temperature each product exists as a mixture of two interconverting boat conformers **A** and **E** (Scheme 10).



Scheme 10. ¹H NMR spectrum (500 MHz, CDCl₃/CS₂) of the reaction products from the intermolecular competition between **13-d₀**/**13-d₃**.

Conformer **A** possesses a pseudoaxial hydroxyl group, while conformer **E** possesses a pseudoequatorial hydroxyl group and they slowly exchange on the NMR time scale (Scheme 10). These conformers (k_H -**A** and k_H -**E** or k_D -**A** and k_D -**E**) exhibit distinguishable ¹H NMR chemical shifts, where one can observe two different sets of peaks one for each isomer. On the other hand, k_H -**A** and k_D -**A** protons (*i.e.* H_c and H_{c'}) as well as k_H -**E** and k_D -**E** protons (*i.e.* H_f and H_{f'}) resonate at exactly the same frequencies (Scheme 10). According to the integrations of the ¹H NMR peaks, the conformer ratio **A/E** for this specific substrate was 4/6, in agreement with that reported in the literature.¹⁸

According to the spectrum displayed in Scheme 10 the integrals of H_f, H_{f'} and H_g absorptions for the **E** conformer can be determined by solving the following equations:

$$H_f + H_{f'} = 2.02 \quad (1)$$

$$H_g = H_f = 1.00 \quad (2)$$

Thus, by combining equations (1) and (2), the product ratio **16-d₀**/**16-d₂** can be easily determined. The ratio of these products, which is the result of intermolecular isotopic competition between **13-d₀** and **13-d₃**, is proportional to the kinetic isotope effect k_H/k_D . Thus the ratio of the integrals of the signals H_f/ H_{f'} for both **E** conformers, determines the isotope effect $k_H/k_D = 0.98 \pm 0.04$.

Identical result is obtained if instead of the peaks of the **E** conformer we use those of the **A** conformer. Working the same way, inter- and intramolecular KIEs for the rest of the substrates

shown in Scheme 6, were measured. The k_H/k_D determined values are shown in Table 1. Notably, in the rest of the cases the ¹H NMR spectra of the reaction products are much simpler since for substrates **14** and **15** formation of a sole conformer is thermodynamically favored (see SI).

Table 1. Intra- and intermolecular kinetic isotope effects.

Substrate	k_H/k_D [a]	Type
13-d₀ / 13-d₃	0.98 ± 0.04	inter
14-d₀ / 14-d₂	0.63 ± 0.03	inter
15-d₃	0.83 ± 0.03	intra
15-d₀ / 15-d₆	0.65 ± 0.03	inter

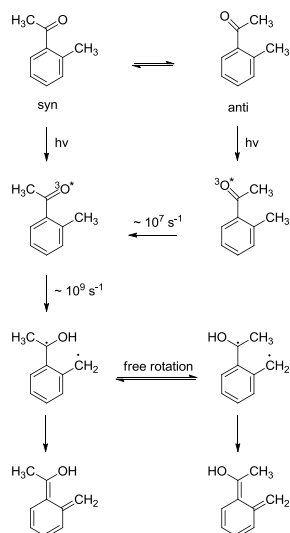
[a] Determination of k_H/k_D by integration of the proper ¹H NMR signals of the cycloaddition products.

The absence of a normal isotope effect ($k_H/k_D > 1$) dictates that there is no C–H or C–D bond breaking in the rate determining step of the reaction. Consequently, according to hypothesis (a) discussed earlier, photoenolization of the *o*-alkyl substituted benzaldehyde to the intermediate α -hydroxy-*o*-quinodimethane (Scheme 5) cannot be the rate-limiting step of the reaction.

The inverse isotope effects measured in all the cases, initially could lead to the conclusion that it is the [4+2] cycloaddition step that determines the reaction rate [hypothesis (b)]. However, if this had been the case, similar values would have been measured for the intermolecular competitions **13-d₀**/**13-d₃** and **15-d₀**/**15-d₆** as well as for the intramolecular competition in **15-d₃**. Therefore, it seems that there is another factor that plays a more significant role in the reaction rate and determines the k_H/k_D product ratio.

The *o*-methylacetophenone photoenolization mechanism proposed by Small and Scaiano, is presented in Scheme 11.^[14] This mechanism is the same as the generic one discussed in Scheme 2, however, at this point we would like to stress some significant details. *o*-Methylacetophenone in its ground state exists as a mixture of two conformers, *syn* and *anti*, in dynamic equilibrium with each other. Upon irradiation, first the singlet and eventually the triplet excited states of these conformers are generated. Subsequently, the triplet state of the *syn* conformation decays to a biradical via intramolecular hydrogen abstraction from the γ position, whereas, the decay of the triplet state of the *anti*-conformer is controlled by bond rotation since first it has to convert to the *syn* conformation through an irreversible bond rotation and then undergo hydrogen atom

abstraction. As a result, the biradical is always formed in the *syn* conformation, but then, the rotation barrier for the interconversion between *syn* and *anti* biradicals is too low that both enols are eventually formed.^[14]



Scheme 11. Photoenolization mechanism for *o*-methylacetophenone.

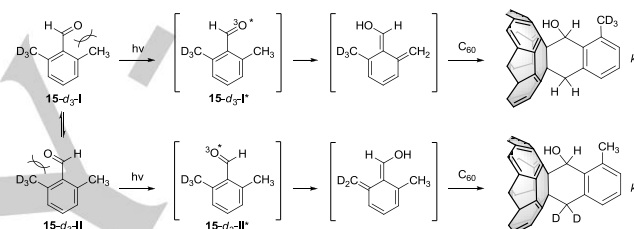
Wagner and co-workers have calculated rate constants for both the intramolecular hydrogen abstraction (k_e) and the rotation around the $C_{\text{aromatic}}-C_{\text{carbonyl}}$ bond (k_r) for several *o*-alkyl ketones in benzene and in *tert*-butyl alcohol.^[11a] Thus, the reaction rate for a hydrogen abstraction is on the order of 10^9 s^{-1} , while $C_{\text{aromatic}}-C_{\text{carbonyl}}$ bond rotation is two orders of magnitude slower ($k_r = \sim 10^7 \text{ s}^{-1}$). Significantly, in their work they conclude that the rotation around the $C_{\text{aromatic}}-C_{\text{carbonyl}}$ bond in the excited state is the rate determining step for the photoenolization of the *anti*-conformer.

Accordingly, in the present study of the photocycloaddition reaction, the rotation between $C_{\text{aromatic}}-C_{\text{carbonyl}}$ bond in the excited triplet state of these carbonyl substrates occurs much slower than γ -hydrogen abstraction. Therefore, it seems reasonable to assume that the above mentioned bond rotation is the reaction limiting step and dictates the k_H/k_D product ratio. In the following paragraphs we will explain the isotope effects measured in this study (summarized in Table 1) utilizing the above statement.

In the case of substrate **15-d₃**, its photochemical addition to C_{60} can be described as shown in Scheme 12, following our previous discussion (Scheme 11). **15-d₃** in its ground state consists of two conformers, **15-d₃-I** and **15-d₃-II** in thermodynamic equilibrium that can lead to photoenolization reaction products. Due to steric hindrance neither of those two

structures is planar, but instead, the carbonyl group is deflected out of the plane of the benzene ring as a consequence of strain in the ground state. Indeed, the MP2 6-311++G** calculation method showed a 20.8° deflection of the carbonyl group out of the plane of benzene (see SI, S19).

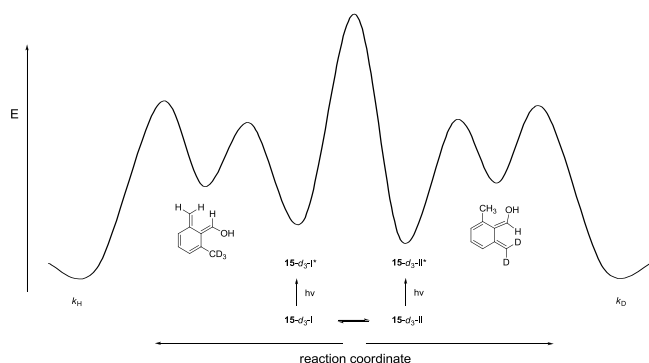
In **15-d₃-I** the oxygen atom is *syn* to the $-CH_3$ group while in **15-d₃-II** is located *syn* to the $-CD_3$ group. The ratio of those two conformers is different from unity since enhanced steric hindrance in **15-d₃-I** (longer C–H bonds, bulkier methyl group)^[22, 23] as compared to **15-d₃-II** (shorter C–D bonds) makes it less stable than **15-d₃-II** (Scheme 12). Thus, the **15-d₃-II** conformation is more populated than the **15-d₃-I** and the same is the case for the excited singlet and triplet states of the molecule as well as the biradicals formed after the intramolecular hydrogen abstraction.



Scheme 12. Photochemical addition of **15-d₃** with C_{60} .

Upon irradiation of the reaction mixture, excited triplet states **15-d₃-I*** and **15-d₃-II*** are generated and they undergo enolization to give the corresponding enols (Scheme 12). According to what we mentioned before, hydrogen abstraction in **15-d₃-I*** and **15-d₃-II*** should happen so fast that no interconversion between these two triplets (via bond rotation) can take place. **15-d₃-I*** leads exclusively to k_H product whilst **15-d₃-II*** gives exclusively k_D (Scheme 12). Consequently, the **15-d₃-I*/15-d₃-II*** ratio determines the product ratio (k_H/k_D). The **15-d₃-I*/15-d₃-II*** ratio is proportional to the **15-d₃-I/15-d₃-II** ratio of the ground state. We can assume, without any significant error, that the initial **15-d₃-I/15-d₃-II** ratio is translated into the final k_H/k_D product ratio. Such cases are known in the literature as non-Curtin-Hammett cases.^[24] Thus, according to the conclusion made in the previous paragraph that **15-d₃-II** conformation is more populated than the **15-d₃-I**, we conclude that the k_D product will be formed at a greater percentage than the k_H . This is how the significant inverse kinetic isotope effect ($k_H/k_D = 0.83$) can be satisfactorily rationalized. In Scheme 13 the proposed energy diagram of the reaction is presented. In this diagram, we want to qualitatively show that the $C_{\text{aromatic}}-C_{\text{carbonyl}}$ bond rotation barrier,

i.e. **15-d₃-I** to **15-d₃-II** interconversion, is significantly higher than any other reaction barrier (photoenolization or [4+2] cycloaddition) that leads to the final products.



Scheme 13. The proposed energy versus reaction coordinate diagram for the photocycloaddition reaction of **15-d₃** with C₆₀.

In the case of the intermolecular competition between **15-d₀** and **15-d₆**, rotation around the C_{aromatic}–C_{carbonyl} bond again plays a crucial role in the ratio of the k_H/k_D and k_D products, however, in this case via a slightly different way.

As we mentioned above, due to steric hindrance between oxygen and –CH₃ and –CD₃ groups, the C=O double bond is out of the plane of the aromatic ring. Upon excitation of the carbonyl group in the singlet and then the triplet state, rotation around the C_{aromatic}–C_{carbonyl} bond brings the oxygen in the vicinity of one the –CH₃ or –CD₃ groups so that the molecule adopts the right geometry that allows the excited carbonyl group to abstract a γ -hydrogen or deuterium. The rotation barrier in **15-d₀** is higher than in **15-d₆** because six C–H bonds induce larger steric hindrance than six C–D bonds. Thus, rotation in **15-d₆** occurs faster than in **15-d₀**, and consequently, deuterated molecules adopt faster the right geometry to give the abstraction reaction faster than the protonated ones, that is, **15-d₆** reacts faster than **15-d₀** leading to the observation of a large inverse kinetic isotope effect ($k_H/k_D = 0.65$).

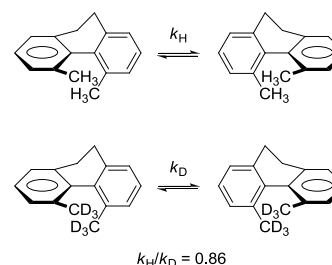
The same is the case with the intermolecular competition of the **14-d₀**/**14-d₂** couple. Substrate **14** in its ground state exists mainly in the *anti* conformation mentioned above for *o*-methylacetophenone (Scheme 11). C_{aromatic}–C_{carbonyl} bond rotation, similarly to compound **15**, is faster in the deuterated substrate (**14-d₂**) than in the protonated one (**14-d₀**) and as a result, photoenolization reaction goes faster for **14-d₂** and therefore k_D product forms faster than k_H .

Interestingly, in substrate **14** there is only one *ortho* substituent (ethyl group) compared to substrate **15** which bears two *ortho* methyl groups. Vibrations involving C–H bonds have higher zero

point energy (ZPE) than those involving the corresponding C–D bonds. In the case of a “crowded” transition state, this difference increases, leading to an inverse remote steric isotope effect, $k_H/k_D < 1$.^[22b] The inverse IE measured between **14-d₀** and **14-d₂** competition is similar to the one found between **15-d₀** and **15-d₆** ($k_H/k_D = 0.63$ and 0.65 respectively). These results indicate that substrates **14** and **15** exhibit similar energy differences between zero point energies and the corresponding transition states.

The close relation between the difference in the rotation barriers of the protonated and deuterated species and the isotope effect measured can be further corroborated by substrate **13**. In this case the isotope effect for **13-d₀**/**13-d₃** is close to unity. Here, the steric hindrance is considerably attenuated and the rotation barriers of **13-d₀** and **13-d₃** are almost identical. That causes **13-d₀** and **13-d₃** to react with the same rate. To conclude, the smaller the difference in the rotation barrier between the two species the less inverse the isotope effect is.

The significant inverse H/D kinetic isotope effects measured in most of the cases above were explained based on the enhanced steric hindrance induced by a group of C–H bonds compared to the shorter C–D bonds that causes conformational changes within the molecule to decelerate. Such cases of conformational kinetic isotope effects emanating from steric restrictions are rare and are manifested only under conditions of severe overcrowding. A few examples have been reported previously.^[25] Perhaps the most impressive example has been reported many years ago by Mislow and coworkers.^[25a] They observed that sterically congested 9,10-dihydro-4,5-dimethylphenanthrenes bearing two trideuteriomethyl groups (Scheme 14) undergo racemization 1.16 times faster than their nondeuterated counterparts in benzene at room temperature. In this case, an inverse steric isotope effect was measured and was found to be equal to $k_H/k_D = 0.86$ (Scheme 14).



Scheme 14. Steric hydrogen isotope effect in the racemization rate of 9,10-dihydro-4,5-dimethylphenanthrene.

Conclusions

To summarize, the rotation around the C_{aromatic}–C_{carbonyl} single bond that, in the excited triplet state of *o*-alkyl carbonyl compounds, is two orders of magnitude slower than the intramolecular hydrogen abstraction, is the rate limiting step for the photocycloaddition reaction of these compounds with C₆₀. Our findings here demonstrate that neither a C–H (or C–D) bond breaking nor a change in hybridization from sp² to sp³ is the rate determining step of the reaction. The intramolecular hydrogen abstraction during the photoenolization step and the subsequent [4+2] cycloaddition proceed fast and efficiently. In fact, it is the high efficiency of these processes that enables the formation of the *o*-quinodimethane-C₆₀ adducts. C₆₀ in solution absorbs very strong in the UV-Vis, while the photoenolizable species, *i.e.* the aromatic carbonyl compounds, absorb only a very small percentage of the incident light, however, this is still enough for this transformation to take place.

Experimental Section

General Considerations. Proton and Carbon nuclear magnetic resonance (¹H NMR and ¹³C {¹H} NMR) spectra were recorded on a Bruker AMX-500 MHz spectrometer, in CDCl₃ or CDCl₃/CS₂ solutions. Chemical shifts are reported in ppm downfield from Me₄Si, by using the residual solvent peak as internal standard. High performance liquid chromatography (HPLC) analyses were carried out on a Cosmosil 5C18-MS-II (4.6 ID × 250 mm) reverse phase column with detection at 310 nm. A mixture of toluene/acetonitrile (50/50) was used as eluent at 1 ml/min flow rate. TLC was carried out on SiO₂ (silica gel F₂₅₄). Flash column chromatography was carried out on SiO₂ (silica gel 60, SDS, 230-400 mesh ASTM). Evaporation of the solvents was accomplished with a rotary evaporator or by high vacuum distillation.

All photochemical reactions were carried out in an ice bath using a 300 W Xenon Cermax lamp as the light source and a Pyrex filter (> 290 nm wavelength). The distance of the light source from the reaction vessel was 13 cm.

Diethyl ether and tetrahydrofuran were distilled over Na under N₂, in presence of benzophenone, prior to use. Benzene and dichloromethane were distilled under N₂ over Na and P₂O₅ respectively and stored over pre-dried molecular sieves 4 Å for at least 24 h prior to use. Commercially available reagents and solvents that didn't need to be dry were used as received without further purification.

Substrate synthesis.

1. Synthesis of *o*-tolualdehyde-*d*₃ (**13-d**₃).

Starting from *o*-bromobenzaldehyde, **13-d**₃ was prepared according to the following three steps:

a) Protection of the carbonyl group in *o*-bromobenzaldehyde.

o-Bromobenzaldehyde (2.5 g, 13.5 mmol), ethylene glycol (2 mL) and *p*-TsOH (0.1 g) were mixed in 50 mL toluene and the mixture was refluxed for 3 h. Next, an additional 4 mL of ethylene glycol were added and heating was continued for an additional 14 h. Reaction progress was monitored by gas chromatography (GC) where it was observed that after the consumption of 85% of the starting material, the reaction practically does not proceed any further. The mixture was cooled down at room temperature and upon addition of diethyl ether (20 mL), was extracted with NaOH 10% (45 mL) and with H₂O (4 × 25 mL). The organic layer was separated and dried over anhydrous MgSO₄. Solvent evaporation gave an oily mixture of the protected product and the starting material. These two compounds were separated by column chromatography (SiO₂, hexane/ethyl acetate 20/1). Pure 2-(2-bromophenyl)-1,3-dioxolane was isolated (2.07 g, yield = 67%). ¹H NMR (500 MHz, CDCl₃): δ = 7.62 (m, 2H), 7.36 (m, 1H), 7.25 (m, 1H), 6.13 (s, 1H), 4.18 (m, 2H), 4.11 (m, 2H).

b) Insertion of a trideuteriomethyl group in the aromatic ring of 2-(2-bromophenyl)-1,3-dioxolane.

2-(2-Bromophenyl)-1,3-dioxolane (2.07 g, 9.0 mmol) and dry THF (40 mL) were placed, under argon, in an oven-dried two-neck round-bottom flask. The solution was cooled down to – 62 °C and then, 12.5 mL (20 mmol) of *t*-BuLi solution (1.6 M in hexane) was added dropwise with vigorous stirring. The reaction mixture was stirred at – 62 °C for 40 min until it adopts a yellow color, and subsequently, the temperature was raised to 0 °C and CD₃I (0.8 mL) was added dropwise. The reaction was stirred at room temperature for 14 h and then, appropriate amount of water was added at 0 °C until all the lithium salts (LiI, LiBr) precipitate giving a transparent solution. Next, diethyl ether (30 mL) was added and the mixture was washed with saturated NaCl solution. The organic layer was collected and dried over anhydrous MgSO₄. Solvent evaporation furnished 2-(*o*-tolyl)-1,3-dioxolane-*d*₃ (1.4 g, yield = 93%) that was used in the next step without further purification. ¹H NMR (500 MHz, CDCl₃): δ = 7.56 (m, 1H), 7.3-7.21 (m, 2H), 7.20 (m, 1H), 5.99 (s, 1H), 4.17 (m, 2H), 4.07 (m, 2H).

c) Deprotection of the carbonyl group in 2-(*o*-tolyl)-1,3-dioxolane-*d*₃.

2-(*o*-Tolyl)-1,3-dioxolane-*d*₃ (1.4 g) and THF (40 mL) were placed in a round-bottom flask and then, of HCl 3N (10 mL) was added. After stirring at room temperature for 24 h, diethyl ether (40 mL) was added and the solution was extracted with H₂O (50 mL). The organic layer was dried over anhydrous MgSO₄ and solvent evaporation furnishing the crude product as oil. Purification with column chromatography (SiO₂, hexane/ethyl acetate 7/1) gave pure *o*-tolualdehyde-*d*₃ (**13-d**₃) (0.6 g, yield = 58%) as a colorless oil. ¹H NMR (500 MHz, CDCl₃): δ = 10.26 (s, 1H), 7.79 (d, *J* = 7.6 Hz, 1H), 7.47 (dd, *J* = 11.80, 4.4 Hz, 1H), 7.36 (t, *J* = 7.5 Hz, 1H), 7.25 (d, *J* = 7.5 Hz, 1H); ¹³C NMR (125 MHz, CDCl₃): δ = 192.83 (s), 140.50 (s), 134.20 (s), 133.66 (s), 132.05 (s), 131.77 (s), 126.35 (s), 18.79 (septet, *J* = 19.25 Hz); HRMS (EI-Sector) *m/z*: [M+ H + Na]²⁺ Calcd for C₈H₆D₃NaO²⁺ 147.0734; Found 147.0803.

2. Synthesis of *o*-ethyl-benzaldehyde-*d*₂ (**14-d**₂).

Starting from *o*-bromoacetophenone, **14-d**₂ was prepared according to the following four steps:

a) Reduction of *o*-bromoacetophenone with LiAlD₄.

In an oven-dried two-neck round-bottom flask, LiAlD₄ (0.17 g, 4 mmol) was dissolved in dry diethyl ether (15 mL) under argon and the resulting mixture was vigorously stirred for 15 min. Then, the flask was cooled down to 0 °C and *o*-bromoacetophenone (2 g, 10 mmol) dissolved in dry diethyl ether (15 mL) were added dropwise. The ice bath was removed and the reaction mixture was stirred at room temperature overnight. After that, the solution was cooled down to 0 °C and quenched with 1 mL of H₂O, 1 mL of NaOH 15% and 3 mL of H₂O until all lithium and aluminum salts precipitate as white solids. The solids were filtrated and the filtrate was washed with NaHCO₃ 5%, brine and finally dried over anhydrous MgSO₄. The solvent was evaporated to give of 1-(2-bromophenyl)ethanol-*d*₁ (1.83 g, yield 90%). ¹H NMR (500 MHz, CDCl₃): δ = 7.62 (m, 1H), 7.53 (m, 1H), 7.37 (m, 1H), 7.15 (m, 1H), 1.97 (br s, OH), 1.50 (s, 3H).

b) Reduction of 1-(2-bromophenyl)ethanol-*d*₁ with Et₃SiD.^[26]

In an oven-dried two-neck round-bottom flask, 1-(2-bromophenyl)ethanol-*d*₁ (1.2 g, 6 mmol) was dissolved in dry dichloromethane (20 mL) under argon. The solution was cooled down to 0 °C and then, Et₃SiD (1.9 mL, 12 mmol) was added dropwise followed by the addition of BF₃/Et₂O solution (7.5 mL, 30 mmol). Subsequently, the reaction mixture was stirred at room temperature for 1 h. During that time significant amount of heat was released. The reaction was quenched at 0 °C by addition of aqueous solution NaOH 10% (2.5 mL) under vigorous stirring. After 15 min., diethyl ether (50 mL) was added and the mixture was washed with saturated NaHCO₃ solution and finally with brine. The organic layer was collected, dried over anhydrous MgSO₄ and the solvent was evaporated to give pure 2-ethyl-bromobenzene-*d*₂ (1.1 g, yield = 99%). ¹H NMR (500 MHz, CDCl₃): δ = 7.55 (m, 1H), 7.26 (m, 2H), 7.07 (m, 1H), 1.24 (br s, 3H).

c) Preparation of 2-ethyl-benzylalcohol-*d*₂(**13-d**₂)

In an oven-dried two-neck round-bottom flask, 2-ethyl-bromobenzene-*d*₂ (1.1 g, 6 mmol) was dissolved in dry THF (30 mL) under argon. The reaction mixture was cooled to –62 °C and *n*-BuLi solution (C = 1.1 M in hexanes) (11 mL, 12 mmol) was added dropwise to give the solution an intense orange color indicative of the formation of the anion on the aromatic ring (due to *ortho* metalation). The reaction was stirred at –62 °C for an additional 30 min and then, formaldehyde (0.21 g, 7 mmol) was added at 0 °C. Stirring was continued at room temperature for 40 min. At the end, the orange color of the solution completely disappeared. The reaction mixture was cooled to 0 °C and water was added to precipitate lithium salts leaving a transparent solution. Next, diethyl ether (30 mL) was added under vigorous stirring and the solution was extracted with brine. The organic layer was separated, dried over anhydrous MgSO₄ and the solvent was removed to obtain pure 2-ethyl-benzylalcohol-*d*₂ (0.4

g, yield = 49%). ¹H NMR (500 MHz, CDCl₃): δ = 10.26 (s, 1H), 7.79 (d, *J* = 7.6 Hz, 1H), 7.47 (dd, *J* = 11.80, 4.4 Hz, 1H), 7.36 (t, *J* = 7.5 Hz, 1H), 7.25 (d, *J* = 7.5 Hz, 1H); ¹³C NMR (125 MHz, CDCl₃): δ = 192.83 (s), 140.50 (s), 134.20 (s), 133.66 (s), 132.05 (s), 131.77 (s), 126.35 (s), 18.79 (septet, *J* = 18.75 Hz); HRMS (ESI Orbitrap) *m/z* [*M* + H - H₂O]⁺ Calcd for C₉H₉D₂⁺ 121.0986; Found 121.0980.

d) Oxidation of 2-ethyl-benzylalcohol-*d*₂ to 2-ethyl-benzaldehyde-*d*₂ (**14-d**₂) (Swern oxidation).^[27]

In an oven-dried two-neck round-bottom flask, oxalyl chloride [(COCl)₂] (520 μL, 6 mmol) and dry dichloromethane (CH₂Cl₂) (15 mL) were mixed under argon. The solution was cooled to –78 °C and dimethyl sulfoxide (DMSO) (570 μL, 8 mmol) dissolved in 15 mL of dry CH₂Cl₂ was added. Reaction was stirred for 10 min and subsequently, 2-ethyl-benzylalcohol-*d*₂ (0.4 g, 3 mmol) dissolved in 10 mL of dry CH₂Cl₂ was added. The resulting solution was stirred at –78 °C for an additional 20 min and then, triethylamine (Et₃N) (3 mL, 22 mmol) was added. The reaction mixture was then stirred at room temperature for 30 min. Water was added next, and the aqueous phase was separated and washed with diethyl ether. The two organic phases were combined together, washed with brine and dried over anhydrous MgSO₄. The solvent was removed *in vacuo* to give 0.4 g of crude product which was further purified by column chromatography (SiO₂, hexane/ethyl acetate 8/1) to give 145 mg of **14-d**₂. ¹H NMR (500 MHz, CDCl₃): δ = 10.28 (s, 1H), 7.83 (dd, *J* = 7.7, 1.4 Hz, 1H), 7.51 (td, *J* = 7.5, 1.5 Hz, 1H), 7.36 (td, *J* = 7.6, 1.1 Hz, 1H), 7.29 (d, *J* = 7.7 Hz, 1H), 1.25 (s, 3H); ¹³C {¹H} NMR (125 MHz, CDCl₃): δ = 192.40 (s), 146.99 (s), 133.95 (s), 133.50 (s), 131.75 (s), 130.22 (s), 126.37 (s), 25.04 (quintet, *J* = 20.00 Hz), 16.13 (s); HRMS (EI-Sector) *m/z* [*M* + H]⁺, calcd for C₉H₉D₂O⁺: 137.0935; Found 137.0930.

3. Synthesis of 2,6-dimethylbenzaldehyde-*d*₃ (**15-d**₃).^[19]

Starting from the commercially available *o*-tolualdehyde (**13-d**₆), **15-d**₃ was prepared in a one-pot reaction according to the following step:

In an oven-dried round-bottom flask, piperidine (0.28 g, 3.3 mmol) was dissolved in dry benzene (10 mL) under argon. Then, *n*-BuLi solution (1.2 M in hexane) (2.8 mL, 3.3 mmol) was added dropwise and the solution was stirred at room temperature for 15 min. Subsequently, *o*-tolualdehyde (**13-d**₆) (0.36 g, 3 mmol) was slowly added and the resulting mixture was stirred for 15 min. After the dropwise addition of *n*-BuLi solution (7.5 mL, 9 mmol), the reaction was refluxed at 80 °C for 15 h. The reaction mixture was cooled to room temperature, dry THF (10 mL) was added, and then, methyl iodide-*d*₃ (CD₃I) (1.12 mL, 18 mmol) was added dropwise at –78 °C. The resulting mixture was stirred to room temperature, poured into 50 mL of cold HCl 10% under stirring, extracted with diethyl ether (60 mL), washed with brine and dried over anhydrous MgSO₄. The solvents were removed *in vacuo* to give the crude product that was further purified by column chromatography (SiO₂, hexane) affording 2,6-dimethylbenzaldehyde-*d*₃ (**15-d**₃) (0.2 g, yield = 48%). ¹H NMR (500 MHz, CDCl₃): δ = 10.65 (s, 1H), 7.35 (dd, *J*₁ = *J*₂ = 7.5 Hz, 1H), 7.11 (d, *J* = 7.5 Hz, 2H), 2.64 (s, 3H); ¹³C NMR (125 MHz, CDCl₃): δ

= 193.66 (s), 141.19 (s), 133.03 (s), 129.74 (s), 127.85 (s), 20.51 (s); (after removing ^{13}C absorptions of a small amount of the corresponding acid); HRMS (EI-Sector) m/z : $[M + \text{H}]^+$ Calcd for $\text{C}_9\text{H}_8\text{D}_3\text{O}^+$ 138.0998; Found 138.0993.

4. Synthesis of 2,6-dimethylbenzaldehyde- d_6 ($15-d_6$).^[19]

$15-d_6$ was prepared in a one-pot reaction from $13-d_6$ following exactly the same procedure described above for the synthesis of $15-d_3$. Methyl iodide (CH_3I) (1.12 mL, 18 mmol) instead of CD_3I was used in this case, whereas the quantities of all the other reagents remained the same. $15-d_6$ was isolated in 50% yield (0.2 g). ^1H NMR (500 MHz, CDCl_3): δ = 10.63 (s, 1H), 7.32 (t, J = 7.5 Hz, 1H), 7.09 (d, J = 7.5 Hz, 2H), 2.61 (s, 6H).

5. Synthesis of 2,6-dimethylbenzaldehyde- d_6 ($15-d_6$).^[19]

$15-d_6$ was prepared in a one-pot reaction from $13-d_3$ following exactly the same procedure described above for the synthesis of $15-d_3$. *o*-Tolualdehyde- d_3 ($13-d_3$) (0.37 g, 3 mmol) was used in this case instead of $13-d_6$, whereas the quantities of all the other reagents remained the same. $15-d_6$ was isolated in 50% yield (0.21 g). NMR (500 MHz, CDCl_3): δ 10.65 (s, 1H), 7.35 (dd, $J_1 = J_2 = 7.5$ Hz, 1H), 7.11 (d, J = 7.5 Hz, 2H), 2.64 (s, 3H); ^{13}C NMR (125 MHz, CDCl_3): δ = 193.65 (s), 141.07 (s), 133.02 (s), 129.72 (s), 127.83 (s), 19.70 (septet, 2C, J = 20.00 Hz); HRMS (EI-Sector) m/z : $[M + \text{H}]^+$ Calcd for $\text{C}_9\text{H}_5\text{D}_6\text{O}^+$ 141.1187; Found 141.1181.

General method for the photochemical addition of *o*-alkylbenzaldehydes with C_{60} .

C_{60} (18 mg, 0.025 mmol) was dissolved in 50 mL benzene in an oven-dried round-bottom flask, and then, a 3- or 5-fold excess of the deuterated carbonyl compound (or an equimolar mixture of deuterated and non-deuterated substrate) was added. The resulting solution was deaerated by bubbling a stream of argon through under continuous stirring for 30 min in the dark. Removal of molecular oxygen is crucial because in the presence of C_{60} , which is a highly efficient photosensitizer,^[28] singlet oxygen ($^1\text{O}_2$) can be generated. This species can react easily either with the aromatic substrates or with C_{60} itself leading to undesired oxygenated products. The reaction solution was placed in an ice bath and irradiated with a xenon lamp (VariacEimacCermax 300W). The distance of the light source from the reaction vessel was 13 cm. The reaction progress was monitored with high performance liquid chromatography (HPLC). The color of the solution changed from deep purple to brown, indicative of the formation of fullerene adducts. Irradiation of the sample was interrupted when roughly 40% of C_{60} was consumed, monitored by HPLC chromatography. Further irradiation leads to an increase in the percentage of multiadducts. For product isolation, most of the benzene was evaporated and the remaining solution was column chromatographed (SiO_2 , toluene/hexane 4/1). Unreacted C_{60} elutes first as a purple band and then follows the monoadduct brown band. The latter band was collected and the solvents were removed to give a brown solid.

Kinetic Isotope Effects Measurements

For the measurement of the kinetic isotope effects, the photochemical reactions of C_{60} with either equimolar mixtures of $13-d_0$ and $13-d_3$, $14-d_0$ and $14-d_2$, $15-d_0$ and $15-d_6$ or substrate $15-d_3$ were realized according to the method described above. The equimolar ratio of the deuterated and nondeuterated counterparts was confirmed based on the ^1H NMR spectra of those mixtures.

As described in the main text, the kinetic isotope effects were calculated from the ratio of the k_{H} and k_{D} products, determined from their ^1H NMR spectra, that equals the $k_{\text{H}}/k_{\text{D}}$ ratio of the rate constants. The corresponding spectroscopic data are reported below (for the NMR spectra and the structures of the fullerene adducts see the SI of this paper).

Intermolecular KIE from the competition in the $13-d_0/13-d_3$ couple.

Both k_{H} and k_{D} products (see also scheme 9) appear as a mixture of the **A** and **E** conformers. ^1H NMR (500 MHz, $\text{CDCl}_3/\text{CS}_2$): δ = 7.96 (m, 1H of $k_{\text{H}}\text{-E}$ and 1H of $k_{\text{D}}\text{-E}$), 7.80-7.50 (m, 3H of $k_{\text{H}}\text{-E}$, 3H of $k_{\text{D}}\text{-E}$, 4H of $k_{\text{H}}\text{-A}$ and 4H of $k_{\text{D}}\text{-A}$), 6.51 (d, J = 6.5 Hz, 1H of $k_{\text{H}}\text{-E}$ and 1H of $k_{\text{D}}\text{-E}$), 6.38 (s, 1H of $k_{\text{H}}\text{-A}$ and 1H of $k_{\text{D}}\text{-A}$), 5.63 (d, J = 13.5 Hz, 1H of $k_{\text{H}}\text{-A}$), 4.83 (d, J = 14 Hz, 1H of $k_{\text{H}}\text{-E}$), 4.51 (d, J = 14 Hz, 1H of $k_{\text{H}}\text{-E}$), 4.37 (d, J = 13.5 Hz, 1H of $k_{\text{H}}\text{-A}$), 3.32 (d, J = 7 Hz, OH of $k_{\text{H}}\text{-E}$ and OH of $k_{\text{D}}\text{-E}$), 3.14 (s, OH of $k_{\text{H}}\text{-A}$ and OH of $k_{\text{D}}\text{-A}$). The value of the KIE was calculated from the integrations of the peaks from the **E** conformer at 6.51 ppm ($k_{\text{H}} + k_{\text{D}}$) and at 4.83 ppm (k_{H}). The result is the same if we use the peak integrations from the **A** conformer.

Intermolecular KIE from the competition in the $14-d_0/14-d_2$ couple.

Both k_{H} and k_{D} products adopt only the **E** conformation. ^1H NMR (500 MHz, $\text{CDCl}_3/\text{CS}_2$): δ = 7.96 (m, 1H of k_{H} and 1H of k_{D}), 7.72-7.62 (m, 3H of k_{H} and 3H of k_{D}), 6.58 (d, J = 7 Hz, 1H of k_{H} and 1H of k_{D}), 4.70 (q, J = 7 Hz, 1H of k_{H}), 3.23 (d, J = 7 Hz, OH of k_{H} and OH of k_{D}), 2.37 (m, 3H of k_{H} and 3H of k_{D}). The value of the KIE was calculated from the integrations of the peaks at 6.58 ppm ($k_{\text{H}} + k_{\text{D}}$) and at 4.70 ppm (k_{H}).

Intermolecular KIE from the competition in the $15-d_0/15-d_6$ couple.

Both k_{H} and k_{D} products adopt only the **A** conformation. ^1H NMR (500 MHz, $\text{CDCl}_3/\text{CS}_2$): δ = 7.58-7.48 (m, 2H of k_{H} and 2H of k_{D}), 7.41 (m, 1H of k_{H} and 1H of k_{D}), 6.73 (m, 1H of k_{H} and 1H of k_{D}), 5.64 (d, J = 13.7 Hz, 1H of k_{H}), 4.34 (d, J = 13.7 Hz, 1H of k_{H}), 3.09 (br s, OH of k_{H} and OH of k_{D}), 2.72 (s, 3H of k_{H}). The value of the KIE was calculated from the integrations of the peaks at 6.73 ppm ($k_{\text{H}} + k_{\text{D}}$) and at 5.64 or 4.34 ppm (k_{H}).

Intramolecular KIE from the photocycloaddition of $15-d_3$ substrate with C_{60} .

Both k_{H} and k_{D} products adopt only the **A** conformation. ^1H NMR (500 MHz, $\text{CDCl}_3/\text{CS}_2$): δ = 7.58-7.48 (m, 2H of k_{H} and 2H of k_{D}), 7.41 (m, 1H of k_{H} and 1H of k_{D}), 6.72 (m, 1H of k_{H} and 1H of k_{D}), 5.63 (d, J = 13.6 Hz, 1H of k_{H}), 4.33 (d, J = 13.6 Hz, 1H of k_{H}), 3.06 (br s, OH of k_{H} and OH of k_{D}), 2.72 (s, 3H of k_{D}). The value of the KIE was calculated from the

integrations of the peaks at 6.72 ppm ($k_H + k_D$) and at 5.63 or 4.33 ppm (k_H).

Acknowledgements

The research work was co-funded by the Greek Ministry of Education and the European Union through research and education action program PYTHAGORAS II 2005 and IRAKLITOS 2002.

This work was supported by the Hellenic Foundation for Research and Innovation (HFRI) and the General Secretariat for Research and Technology (GSRT), under the HFRI PhD Fellowship grant (GA. no. 4813).

Supplementary Material: ^1H NMR spectra, ^{13}C $\{^1\text{H}\}$ NMR spectra of all new substrates. ^1H NMR spectra of Diels-Alder cycloaddition products of C_{60} with hydroxy-o-quinodimethanes. HRMS spectra of substrates 13- d_3 and 13- d_2 . MP2 6-311++G** calculation method for the geometry of substrate 15- d_3 . Experimental details. This material is available free of charge via the Internet at <http://pubs.acs.org>.

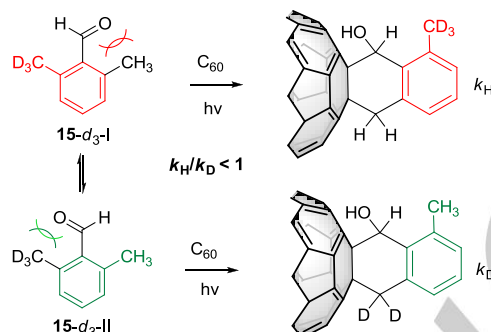
Keywords: C_{60} -functionalization • Photoenolate • Cycloadditions • Mechanism • Isotope Effects

- [1] A. Hirsch and M. Brettreich, *Fullerenes: Chemistry and Reactions*. Eds: Wiley-VCH Verlag GmbH & Co. KGaA, Weinheim, 2005, pp 101.
- [2] T. Tago, T. Minowa, Y. Okada, J. Nishimura, *Tetrahedron Lett.* **1993**, *34*, 8461-8464.
- [3] A. Gügel, A. Kraus, J. Spickermann, P. Belik, K. Müllen, *Angew. Chem., Int. Ed. Engl.* **1994**, *33*, 559-561.
- [4] X. Zhang, C. S. Foote, *J. Org. Chem.* **1994**, *59*, 5235-5238.
- [5] B.M. Illescas, N. Martín, C. Seoane, E. Orti, P. M. Viruela, R. Viruela, A. de la Hoz, *J. Org. Chem.* **1997**, *62*, 7585-7591.
- [6] P. Belik, A. Gügel, J. Spickermann, K. Müllen, *Angew. Chem., Int. Ed. Engl.* **1993**, *32*, 78-80.
- [7] a) U. M. Fernández-Paniagua, B. Illescas, N. Martín, C. Seoane, P. de la Cruz, A. de la Hoz, F. Langa, *J. Org. Chem.* **1997**, *62*, 3705-3710; b) B. González, A. Herrera, B. Illescas, N. Martín, R. Martínez, F. Moreno, L. Sánchez, A. Sánchez, *J. Org. Chem.* **1998**, *63*, 6807-6813.
- [8] J. L. Segura, N. Martín, *Chem. Rev.* **1999**, *99*, 3199-3246.
- [9] N. C. Yang, C. Rivas, *J. Am. Chem. Soc.* **1961**, *83*, 2213.
- [10] a) B. J. Arnold, S. M. Mellows, P. G. Sammes, T. W. Wallace, *J. Chem. Soc., Perkin Trans. 1* **1974**, 401-409; b) P. G. Sammes, *Tetrahedron* **1976**, *32*, 405-422.
- [11] a) P. J. Wagner, C. P. Chen, *J. Am. Chem. Soc.* **1976**, *98*, 239-241.; b) R. Hagg, J. Wirz, P. J. Wagner, *Helv. Chim. Acta* **1977**, *60*, 2595-2607.
- [12] P. J. Wagner, *Pure Appl. Chem.* **1977**, *49*, 259-270.
- [13] P. K. Das, J. C. Scaiano, *J. Photochem.* **1980**, *12*, 85-90.
- [14] R. D. Small Jr, J. C. Scaiano, *J. Am. Chem. Soc.* **1977**, *99*, 7713-7714.
- [15] P. K. Das, M. V. Encinas, R. D. Small Jr, J. C. Scaiano, *J. Am. Chem. Soc.* **1979**, *101*, 6965-6970.
- [16] R. G. W. Norrish, C. H. Bamford, *Nature* **1937**, *140*, 195-196.
- [17] H. Tomioka, M. Ichihashi, K. Yamamoto, *Tetrahedron Lett.* **1995**, *36*, 5371-5374.
- [18] a) Y. Nakamura, K. O-kawa, S. Minami, T. Ogawa, S. Tobita, J. Nishimura, *J. Org. Chem.* **2002**, *67*, 1247-1252; b) K. O-kawa, Y. Nakamura, J. Nishimura, *Tetrahedron Lett.* **2000**, *41*, 3103-3106.
- [19] D. L. Comins, J. D. Brown, *J. Org. Chem.* **1984**, *49*, 1078-1084.
- [20] N. Chronakis, M. Orfanopoulos, *Org. Lett.* **2001**, *3*, 545-548.
- [21] A. Streitwieser Jr., R. H. Jagow, R. C. Fahey, S. Suzuki, *J. Am. Chem. Soc.* **1958**, *80*, 2326-2332.
- [22] For theory and examples of KIEs see: a) L. Melander, W. H. Saunders, "Reaction Rates of Isotopic Molecules" Wiley-Interscience, New York, 1980; b) K. B. Carpenter, *Determination of Organic Reaction Mechanisms. Isotope Effects*: John Wiley & Sons: New York, 1984; Chapter 5; c) D. Wade, *Chem.-Biol. Interact.* **1999**, *117*, 191-217.
- [23] K. Kuchitsu, L. S. Bartell, *J. Chem. Phys.* **1962**, *36*, 2470 - 2481.
- [24] E. L. Eliel, S. H. Wilen, *Stereochemistry of Organic Compounds*; John Wiley & Sons Co., Inc.: New York: **1994**; Chapter 10, pp 647-655.
- [25] a) K. Mislow, R. Graeve, A. J. Gordon, G. H. Wahl Jr., *J. Am. Chem. Soc.* **1964**, *86*, 1733-1741; b) L. Melander, R. E. Carter, *J. Am. Chem. Soc.* **1964**, *86*, 295-296; c) T. Filder, C. A. Schalley, *Angew. Chem., Int. Ed. Engl.* **2003**, *42*, 2258-2260; d) J. S. Mugridge, R. G. Bergman, K. N. Raymond, *Angew. Chem., Int. Ed. Engl.* **2010**, *49*, 3635-3637.
- [26] J. L. Fry, M. Orfanopoulos, M. G. Adlington, W. R. Dittman Jr.; S. B. Silverman, *J. Org. Chem.* **1978**, *43*, 374-375.
- [27] H. Oikawa, T. Kobayashi, K. Katayama, Y. Suzuki, A. Ichihara, *J. Org. Chem.* **1998**, *63*, 8748-8756.
- [28] a) J. W. Arbogast, P. Aleksander, A. P. Darmanyan, C. S. Foote, F. N. Diederich, R. L. Whetten, Y. Rubin, M. M. Alvarez, S. J. Anz, *J. Phys. Chem.* **1991**, *95*, 11-12; b) M. Orfanopoulos, S. Kambourakis, *Tetrahedron Lett.* **1994**, *35*, 1945-1948.

FULL PAPER

Photoenol reactive intermediates add to C_{60} , producing stable [4+2] fullerene adducts.

A mechanistic approach for this reactivity of C_{60} is provided, based mainly on intra and intermolecular kinetic isotope effects (KIEs) studies.

**Photoenolates of $[C_{60}]$ Fullerene**

*Manolis M. Roubelakis, Nikitas G. Malliaros, and Michael Orfanopoulos**

Page No. – Page No.

A Mechanistic Study of the Diels-Alder Cycloaddition of C_{60} with Photochemically Generated Hydroxy-*o*-quinodimethanes.

A facile functionalization governed by steric factors